# Rubidium vapor holography for noncontact adaptive detection of ultrasound

Nikolai Korneev,[1,*] P. Rodríguez-Montero,[1] and Olena Benavides[2]

[1]*Instituto Nacional de Astrofísica, Óptica y Electrónica, Luis Enrique Erro 1, Tonantzintla, Puebla 72840, Mexico*
[2]*Universidad Autónoma del Carmen, Ciudad del Carmen, Campeche 24180, Mexico*
[*]*Corresponding author: korneev@inaoep.mx*

Received April 1, 2009; revised May 19, 2009; accepted May 21, 2009;
posted May 28, 2009 (Doc. ID 109601); published June 23, 2009

We describe an adaptive interferometer based on rubidium vapor, which combines a good signal-to-noise ratio with a high cutoff frequency of ~1 MHz. These features can be useful for optical detection of ultrasound generated in diffusely scattering objects in the presence of strong environmentally produced vibrations. © 2009 Optical Society of America

*OCIS codes:* 120.1088, 190.7070, 280.3375.

Several optical methods were proposed for the detection of ultrasound for purposes of industrial quality control [1,2]. For a whole noncontact inspection, the ultrasound excitation in the sample under test is often made with a pulsed laser (laser ultrasonics). The detection in this case is quite demanding, because small surface displacements (<10 nm) of optically rough surfaces have to be detected in a characteristic bandwidth of 10–30 MHz. Unwanted low-frequency vibrations with much larger amplitude are usually present in the environment and must not interfere with the measurement. Adaptive interferometers with photorefractive crystals in a two-wave mixing (TWM) configuration and adaptive photodetectors based on the non-steady-state photoelectromotive force (photo-EMF) effect [3–6] is one of the detection alternatives. In the TWM configuration (Fig. 1), the adequate holographic medium has to combine high diffraction efficiency with fast recording and erasing. For optimal suppressing of environmental factors, the material response time has to be in the microsecond range. For typical cw laser powers, the materials used so far (sillenites and semiconductors) have recording times in the millisecond range, which limits their adaptive properties [5,6]. Adaptive photodetectors based on the non-steady-state photo-EMF effect in semiconductors demonstrate shorter response time, but their signal-to-noise ratio (SNR) is nominally and practically lower than that of the holographic devices based on the TWM configuration [4].

Rubidium vapor is promising for holographic detection of ultrasound, because its sensitivity as a recording medium is 4 orders of magnitude higher than the sensitivity of the fastest photorefractive crystals, the writing time is in the 100 ns range, and the diffraction efficiency can be high (>10%) [7]. Predominantly phase gratings (which allow a linear detection of phase modulated signals) can be written in it with a low power tunable cw semiconductor lasers at resonance with the atomic transition. Rubidium cells have low price and excellent optical quality, and the properties of the material do not vary from one cell to another.

Here we report the experimental study of rubidium vapor as a holographic medium for the detection of laser-generated ultrasound in a TWM configuration (see Fig. 1). The principle of its operation is well known for photorefractive samples [3,5,6]. Two interfering waves in a medium with nonlinear response produce a dynamic hologram, which can be regarded as an adaptive multilayer dielectric mirror. Its position inside the material, with respect to the interference fringes, gives an optimal working point in the quadrature, and irregular wavefronts are compensated because of the involved holographic process. For fast displacements of the interference pattern, the hologram remains practically static during the rewriting time, close to its original position. As a result, a transient intensity transfer between the beams is obtained, which is detected by a pair of photodiodes. After the hologram is rebuilt into the new position, the energy transfer between the beams returns to its steady-state value. The ability of adaptive interferometer to compensate for environmentally induced wavefront distortions and slow phase drifts is inversely proportional to the hologram recording time.

The optical setup for our experiment is shown in Fig. 1. Two beams were derived from a tunable semiconductor laser (<50 mW) at a wavelength of 780.24 nm, which is at resonance with the D2 rubidium line. The reference beam and the signal beam were crossing at a small angle (~10 mrad) inside the rubidium cell. We used a 25-mm-long natural rubidium cell (78% of Rb85 and 22% of Rb87 isotopes) placed inside a solenoid. For the operation, the cell was heated to 80°C–150°C. The geomagnetic field compensation

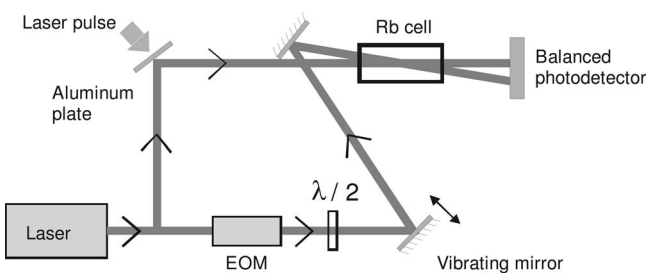


Fig. 1. Experimental setup. EOM, electro-optic phase modulator. The angle between the beams inside the cell is exaggerated for better visibility.

 

was achieved with a mu-metal shield. Beam powers before the cell were 7.1 and 4.3 mW for the reference and signal beams, respectively. Both beams had a diameter of about 1 mm. We performed experiments using various combinations of magnetic fields smaller than 2 G and input polarizations. The best results were obtained for the geometry in which the linear polarizations of the input beams were mutually orthogonal, and the external magnetic field is set to zero. In this geometry, the intensity in the crossing area of the beams is more or less uniform, but the polarization is changing from linear to elliptical and back, following the fringe pattern. The principle of operation is based on the nonlinear effect of self-rotation of elliptically polarized light [8]. In this case the diffraction with polarization rotation is observed. The detailed operation of this particular geometry will be described elsewhere.

As one of the mirrors in the interferometer we used a polished aluminum plate with an ultrasonic piezoelectric transducer attached to it. We could also remove the transducer and apply to the back surface of the plate the pulse of a $Q$-switched Nd:YAG laser (8 ns pulse duration and 500 mJ of energy per pulse). The quality of the polishing was not good enough to obtain an optically flat surface. Indeed the output spot at the photodetector plane typically presented 10–100 speckles depending on the illuminated point on the aluminum plate. To enhance the SNR, we used two identical fast photodiodes with a rise time of 15 ns in a simple balance scheme. The predominant noise factors were the electronic noise of the amplifier and the laser wavelength instability.

We worked with the $Fg=2$ transition of Rb87. For moderate temperatures (lower than 80 °C) the signal is maximal close to the center of this line. For higher temperatures, larger signals are obtained at the red-shifted line edge, because the transmission at the center becomes quite small. The data reported here were obtained at the temperature of 110 °C with the wavelength that gives close to 50% transmission (approximately 0.5 GHz detuning from the line center).

We used an electro-optic phase modulator in the signal arm to calibrate the setup and for fine-tuning the conditions for ultrasound detection. The response of the photodetector pair to the square phase modulation with an amplitude of $\Delta=0.15$ rad is shown in Fig. 2. It is observed that the ac components of the signals at two photodiodes are 180° out of phase and have nearly equal magnitudes. This shows, in particular, that the hologram has a dominant phase component. The signs of the signal for displacements of the interference pattern in different directions are opposite, which means that there is a predominantly linear response to the phase modulation. The linearity of response was confirmed by applying a sinusoidal phase modulation—in the case of linear response there is no distortion in the photodetector signal. The minimal detectable (noise equivalent) phase modulation in a 20 MHz band is 1–2 mrad, corresponding to 0.06–0.12 nm of surface displacement, which is 10–100 times better than the value experimentally achieved with semiconductor photo-EMF

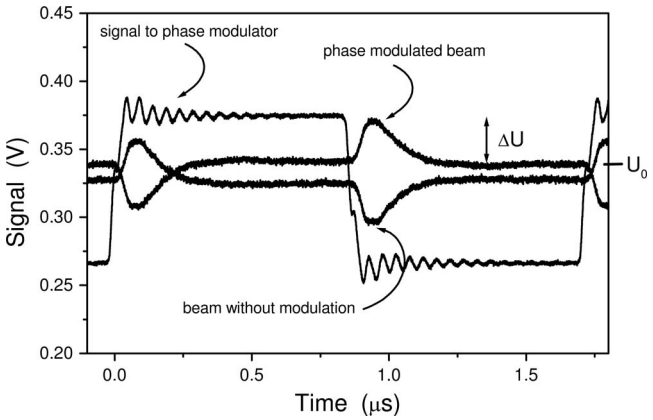


Fig. 2. Response of the two photodetectors to the square wave phase modulation in the signal arm. No averaging is used. The phase modulation amplitude is $\Delta=0.15$ rad. The visible noise is bigger than the actual level because the oscilloscope scale is chosen to show dc components of signals as well as ac.

detectors [9]. This is only three to six times worse than the theoretically achievable sensitivity of such detectors [4] and quite similar to the results reported for the GaAs TWM device [6]. From Fig. 2, the hologram recording time can be estimated as 150 ns (corresponding to the $1/e$ decay). The decay is not strictly exponential, and its particular shape depends on the writing polarizations, magnetic field, and laser wavelength. Using the data in Fig. 2, the diffraction efficiency of the grating can be estimated as well. Since the modulation depth (defined as the $\Delta U/U_0$—see Fig. 2) is proportional to $\sin(\Delta)$, we obtain that the maximal possible modulation depth is $[\sin(0.15)]^{-1} \approx 6.7$ times bigger than the one shown in this graph. Note that we have ~50% of absorption at the working wavelength. The ratio of the diffraction efficiency to the absorption is generally bigger for higher light intensities because of the light-induced transparency. The vapor density grows exponentially with temperature, and both absorption and grating strength are proportional to the density; thus the diffraction efficiency can be strongly enhanced by raising the temperature, with the corresponding growth in absorption.

In Fig. 3 we show the oscilloscope trace for the case when the ultrasonic piezoelectric transducer is attached to the back surface of the aluminum plate (single pulse). The trace obtained when a single shot of Nd:YAG laser impinges on the back surface of the aluminum plate is shown in Fig. 4. Both traces are characteristic for laser ultrasound. In particular, for the laser-generated ultrasound, the arrival of the first wave and the subsequent echoes are clearly distinguishable.

To estimate the adaptive properties of the rubidium vapor as an adaptive holographic medium, we used a vibrating mirror driven by a low-frequency loudspeaker. We could not find any influence for a jamming amplitude up to ~1000 rad at 200 Hz, which was the maximal amplitude we could obtain. In this case, the sinusoidal signal with 5.7 MHz frequency remained constant within a 1% error level.

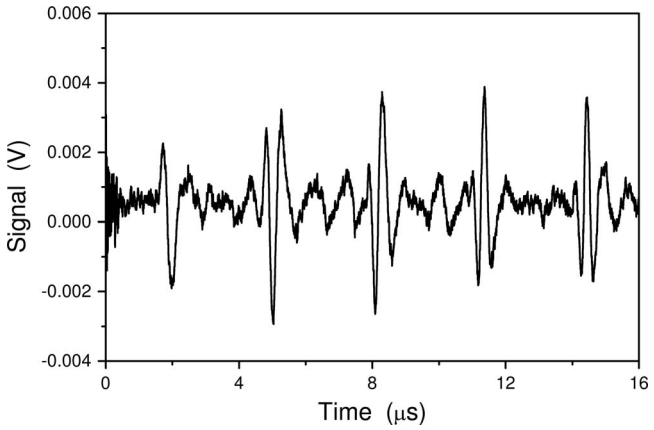


Fig. 3. Differential photodetector signal resulting from a single pulse of the ultrasound transducer attached to the back side of the polished aluminum plate. The signal before the first spike is the electric pickup from the transducer power supply.

The result is compatible with the 1 MHz cutoff frequency of rubidium vapor. This is important if the laser ultrasonic technique is intended for use without special vibration insulation or in a noisy environment.

To investigate the possibility of working with rough surfaces, we replaced the polished aluminum plate with an as-processed rough one. Two lenses with focal distances of 75 and 20 mm were used to focus the beam onto the surface and to collect the reflected light inside the Rb cell. The spot on the plate was about 100 $\mu$m in size and produced strongly speckled output. In this experiment, the phase modulation was produced in the reference beam with the electro-optic modulator—not by the pulsed laser. The output signal, in comparison with the experiment with the polished plate, was about three times smaller. This difference is partly explained by the drop in the collected light power. Thus in another experiment we used a telescopic system and a ground glass plate to produce in the signal beam a speckled structure with a divergence of 15 mrad in a far field. For powers of 4.8 and 0.24 mW for the reference and signal beams, respectively, the measured TWM signal with speckles was ~0.7 of the signal obtained for the same beam powers without speckles. We were limited in our experiments by the cell length (25 mm), which dictates, together with the requirement of sufficient intensity (small beam diameter), rather small angles between the writing beams. In principle, for shorter cells, the writing angles can be made bigger, and the vapor density can be enhanced by raising the temperature. However, one can expect some drop in the diffraction efficiency to absorption ratio for small grating periods, because the time of flight of the rubidium atom through the fringe diminishes. No estimations of this factor, as far as we know, were actually made, and the underlying theory is highly involved.

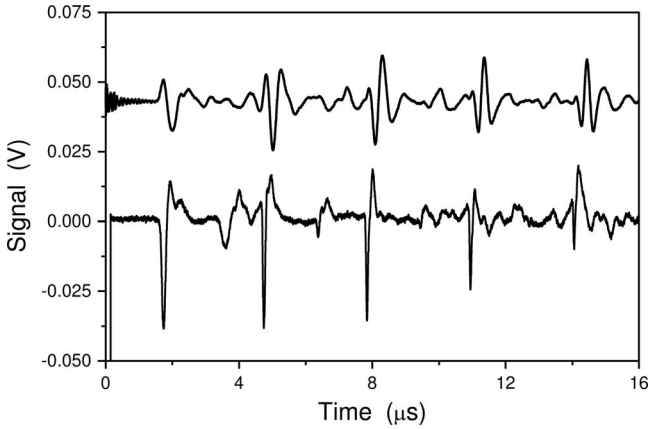


Fig. 4. Trace of the signal after a single laser pulse is applied (lower trace). The signal from the ultrasound transducer averaged over 16 shots is shown for comparison (not to scale, upper trace). Both traces have spikes corresponding to ultrasound wave reflections from the plate surfaces, but for the laser induced pulse the spikes are narrower. The amplitude for the laser-generated first spike is about 40 nm.

In conclusion, the presented experimental data demonstrate that rubidium vapor as a holographic material is highly promising for noncontact detection of ultrasound in the presence of strong low-frequency vibrations. The proposed setup demonstrates good SNR, similar to that of TWM adaptive interferometers, but, different from traditional photorefractive materials, the rubidium vapor has a submicrosecond recording time, which ensures excellent adaptive properties.

This work was done with partial support from CONACYT-SALUD project 2005-01-14012.

## References

1. C. B. Scruby and L. E. Drain, *Laser Ultrasonics: Techniques and Applications* (Hilger, 1990).
2. R. J. Dewhurst and Q. Shan, Meas. Sci. Technol. **10**, R139 (1999).
3. L. Solymar, D. J. Webb, and A. Grunnet-Jepsen, *The Physics and Applications of Photorefractive Materials* (Oxford U. Press, 1996), Chap. 13.
4. S. Stepanov, in *Handbook of Advanced Electronic and Photonic Materials and Devices*, Vol. 2 of Semiconductor Devices, H. S. Nalwa, ed. (Academic, 2001), p. 205.
5. P. Delaye, A. Blouin, D. Drolet, L. A. de Montmorillon, G. Roosen, and J. P. Monchalin, J. Opt. Soc. Am. B **14**, 1723 (1997).
6. B. Campagne, A. Blouin, L. Pujol, and J. P. Monchalin, Rev. Sci. Instrum. **72**, 2478 (2001).
7. N. Korneev and O. Benavides, J. Opt. Soc. Am. B **25**, 1899 (2008).
8. S. M. Rochester, D. S. Hsiung, D. Budker, R. Y. Chiao, D. F. Kimball, and V. V. Yashchuk, Phys. Rev. A **63**, 043814 (2001).
9. P. Rodriguez Montero, S. Stepanov, C. C. Wang, and S. Trivedi, Nondestr. Test. Eval. **21**, 91 (2006).